

Length-scale-dependent vortex-antivortex unbinding in epitaxial $\text{Bi}_2\text{Sr}_2\text{CaCu}_2\text{O}_{8+\delta}$ films

L. Miu*

*Institute of Physics, Johannes Gutenberg University, D-55128 Mainz, Germany
and Kent State University, Department of Physics, Kent, Ohio 44242*

G. Jakob, P. Haibach, Th. Kluge, U. Frey, P. Voss-de Haan, and H. Adrian

Institute of Physics, Johannes Gutenberg University, D-55128 Mainz, Germany

(Received 8 July 1997)

The supercurrent transport properties of epitaxial $\text{Bi}_2\text{Sr}_2\text{CaCu}_2\text{O}_{8+\delta}$ films in zero applied magnetic field were investigated in a temperature interval of ≈ 20 K below the mean-field critical temperature T_{c0} . The modification of the shape of the I - V curves observed by varying the temperature was explained in terms of vortex-fluctuation-induced layer decoupling and vortex-antivortex unbinding, revealing a strong probing-length dependence. The change of the effective dimensionality of thermally excited vortices involved in the dissipation process leads to the appearance of a few characteristic regions in the current-temperature diagram. Above a temperature value $T^* < T_{c0}$, the superconducting layers are decoupled, as predicted by Monte Carlo simulations and renormalization-group analyses. In this region, the resistivity exhibits two-dimensional (2D) behavior corresponding to the superconducting $(\text{CuO}_2)_2$ layers (2D-layer behavior). However, the resistive transition seems to be mainly related to the 2D behavior at the film level. In the sensitivity window of our measurements, finite resistance in the limit of small transport currents was detected to occur above a temperature value $T_c < T^*$, through the dissociation of vortex-string-antivortex-string pairs. By decreasing the temperature and/or by increasing the transport current, the I - V curves in the double logarithmic plot show a clear downward curvature. This can be described in terms of current-induced quasi-2D vortex pair unbinding, with a nonzero critical-current density resulting from the interlayer Josephson coupling. At even lower temperatures and/or higher transport currents, the I - V curves exhibit a crossover from quasi-2D to 2D-layer behavior, due to the decrease of the probing length below the Josephson length, where the interlayer Josephson coupling becomes irrelevant. The temperature dependence of the 2D I - V exponent is in good agreement with recent Langevin simulations of the Coulomb gas model, revealing an anomalous diffusion of vortex fluctuations. [S0163-1829(98)01505-7]

I. INTRODUCTION

The dissipation in transport-current-carrying high-temperature superconductors (HTSC's) in zero external magnetic field occurs at transport currents lower than the depairing critical current. The large intrinsic anisotropy, as in the case of $\text{Bi}_2\text{Sr}_2\text{CaCu}_2\text{O}_{8+\delta}$ (Bi-2212) HTSC, generated by the layered structure, suggests that the thermally excited 2D vortices of opposite helicity in the superconducting Cu-O layers play the essential role.¹ Some transport measurements² signaled features of the Berezinskii-Kosterlitz-Thouless (BKT) transition^{3,4} at the superconducting layer level, but the nonvanishing interlayer Josephson coupling gives rise to a finite critical-current density,⁵⁻⁸ and the picture becomes complex.

For layered superconductors without interlayer Josephson coupling, the interaction between 2D vortices and antivortices depends logarithmically on their separation, even for large values of the latter. Neglecting the magnetic interaction between vortices located in different layers, such systems are good candidates for the occurrence of the BKT transition.¹ Below the Kosterlitz-Thouless transition temperature T_{KT} , the vortices and antivortices are bound in pairs.³ The thermally induced 2D free vortices will be present at $T > T_{KT}$, their creation becoming thermodynamically favorable due to the entropy contribution to the free energy. T_{KT} is the solution of the implicit equation⁴

$$T_{KT} = s\Phi_0^2/[8\pi\lambda^2(T_{KT})\epsilon(T_{KT})\mu_0k_B], \quad (1)$$

where s is the interlayer spacing, λ is the in-plane component of the magnetic penetration depth, and ϵ is the dielectric constant, which incorporates the screening of the interaction energy. If the quenched disorder is irrelevant, the critical current of a 2D system of large extension will be essentially zero, the current-voltage (I - V) characteristics having a power-law dependence, $V \sim I^{\alpha(T)}$. In the classical approach,⁹ the I - V exponent $\alpha(T) = 1 + \text{const}(1/T - 1/T_{c0})$ below T_{KT} , and is expected to exhibit a sudden decrease from 3 to 1 at T_{KT} . Recently, the dynamic properties of 2D vortex fluctuations were investigated through simulations of the 2D Coulomb gas model, in which the vortices were represented by soft disks with logarithmic interaction. It was found that the 2D vortex fluctuations obey intrinsic anomalous dynamics, leading to a different I - V exponent.¹⁰

In the presence of weak interlayer Josephson coupling, the vortex-antivortex interaction energy has a supplementary term, which grows linearly with the vortex separation,⁶ and generates an "intrinsic" critical-current density⁷ $J_c \sim 1 - T/T_{c0}$. In such a situation, no sign of a BKT transition at the level of the superconducting layers should be observed. (With the above term in the vortex interaction energy, the free energy of the system with an independent vortex will increase indefinitely with the characteristic system size, irre-

spective of temperature.) However, for thin film samples, the finite interlayer Josephson coupling makes possible a BKT transition associated with vortex-string pairing.^{11,12} At first sight, this would be in conflict with the form of the I - V curves below the resistive transition reported in Ref. 8, which indicates the existence of a finite critical-current density. The often reported 2D behavior above the resistive transition of HTSC's can be the result of the occurrence of a vortex-fluctuation-induced layer decoupling, as predicted by Monte Carlo simulations^{13,14} and recent renormalization-group analyses.^{15–18} This is understood as a decoupling between vortices in different layers due to the vortices themselves.¹⁴ At the same time, it was found that the Josephson-coupling-mediated term of the in-plane vortex-antivortex interaction energy vanishes above the resistive transition.⁸ However, to associate the resistive transition of the system with the BKT transition at the layer level is in contradiction with the three-dimensional character of the former, appearing in theoretical analyses.¹⁹

In the present work, we investigated the zero-field in-plane supercurrent transport properties of epitaxial Bi-2212 films in a temperature interval of ≈ 20 K below the mean-field critical temperature, in order to gain some further insight into the dissipation process in transport-current-carrying highly anisotropic HTSC's. We found that, in the condition of negligible pinning, the modification of the I - V curve shape with decreasing temperature illustrates the change of the effective dimensionality of the thermally excited vortices. This appears to be temperature and length-scale dependent. For thin film samples, we show that it is possible to distinguish between the 2D-layer properties, the quasi-2D behavior, and the 2D-film behavior. The 2D-layer properties are related to the existence of 2D vortices in the superconducting $(\text{CuO}_2)_2$ layers with logarithmic interaction only. The quasi-2D behavior is the result of thermal excitation of 2D vortices located in the superconducting layers, with both logarithmic and Josephson-coupling-mediated in-plane interactions, whereas the 2D-film behavior is generated by vortex strings parallel to the c axis (threading the whole film), with logarithmic interaction.

II. SAMPLE PREPARATION AND CHARACTERIZATION

The Bi-2212 films (about 400 nm thick) were prepared with a high degree of reproducibility by an *in situ* sputtering method on (100) oriented SrTiO_3 substrates, as described in Ref. 20. The strongly c -axis-oriented growth and in-plane epitaxy were confirmed by x-ray-diffraction studies in a Bragg-Brentano and four circle geometry. The stacking sequence was also investigated by transmission electron microscopy, which revealed a low density of stacking faults. The patterning of the film into a suitable four probe structure was performed by a standard photolithographic technique, and the electrical contacts were obtained by evaporating and annealing silver. We used $1.8 \text{ mm} \times 200 \mu\text{m}$ strips for transport measurements with pulsed and reversed current. The supercurrent transport properties of the as-grown film (Bi-2212ag) were presented in some detail in Ref. 20. A second film (Bi-2212ox), prepared under the same conditions, was supplementary maintained at 600°C for 3 h in 1 kPa oxygen, for a better homogeneity of the oxygen distri-

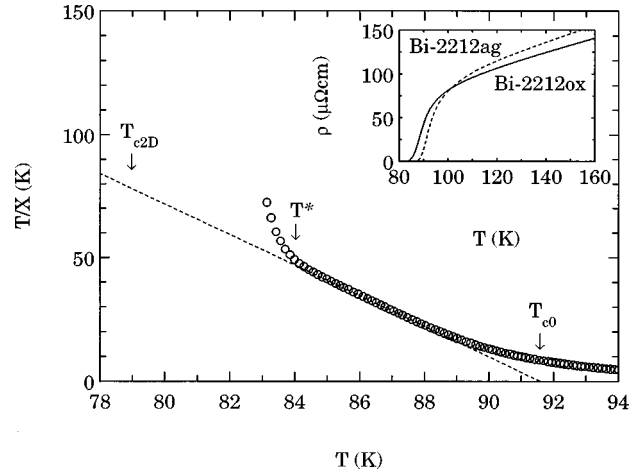


FIG. 1. The resistive data in zero applied magnetic field for the oxygen annealed sample (Bi-2212ox, see inset) plotted as T/X versus T . $X(T)$ was obtained using the experimental $\rho(T)/\rho_n$ data, by means of numerical inversion of Eq. (1) from Ref. 22. ρ_n was determined as the normal-state resistivity at T_{c0} , by iterations. We considered for the temperature dependence of the normal state resistivity the sample resistivity measured at $T > 140$ K linearly extrapolated down to T_{c0} . The dashed line represents the linear fit of the T/X data in the region of 2D-layer behavior. The intersection between the dashed line and the T axis gives $T_{c0} = 91.5$ K, whereas the temperature value for which $X=1$ would be the critical temperature expected in the case of the layered system without interlayer Josephson coupling, $T_{c2D} = 78.9$ K. $T^* \approx 84$ K is the layer decoupling temperature (see text). The inset illustrates the zero-field resistive transitions of the investigated films, for a transport current value $I = 0.1$ mA. Compared with the as-grown film (Bi-2212ag), the oxygen annealed sample (Bi-2212ox) has a lower normal-state resistivity and a reduced T_{c0} value.

bution and a low degree of disorder. This film was thoroughly investigated here and compared with the as-grown film. After the above oxygen annealing, both the resistivity in the normal state and the critical temperature decreased (Fig. 1, inset), and the elemental cell was ‘‘compressed’’ along the c axis by $\approx 0.1\%$. At the same time, the carrier concentration, determined from the Hall constant measured at 150 K, increased by $\approx 10\%$. All these changes indicate a higher doping level for the second film.

III. RESULTS AND DISCUSSION

First, we present the analysis of the resistive transition. As it is known, in the case of highly anisotropic HTSC's, Monte Carlo simulations^{13–14} and renormalization-group analyses^{15–18} revealed the occurrence of a vortex-fluctuation-induced layer decoupling just above the resistive transition, which has been experimentally confirmed.⁸ In these circumstances, the temperature dependence of the electrical resistivity ρ of these materials can be investigated in the framework of the Ginzburg-Landau 2D Coulomb-gas model.^{21–23} This model predicts that certain measurable quantities can only depend on the dimensionless variable $X = T_{CG}(T)/T_{CG}(T_c) = (T/T_c)(T_{c0} - T_c)/(T_{c0} - T)$, where T_{CG} is the Coulomb-gas temperature²¹ and T_c is the critical temperature of the system. One can apply this to the ratio $\rho(T)/\rho_n$, where ρ is the measured resistivity below T_{c0} and

ρ_n is the normal state resistivity. From the above definition of X , in the Ginzburg-Landau treatment of the superfluid density, the ratio T/X should be a linear function of temperature,

$$T/X \sim T_{c0} - T, \quad (2)$$

which can be used for the determination of the mean-field critical temperature, if the variable X is extracted independently. To do this, one makes the assumption that the $\rho(T)$ data follows the universal 2D scaling curve,²² and $X(T)$ is derived from the experimental $\rho(T)/\rho_n$ data by means of numerical inversion of Eq. (1) from Ref. 22 (see, for example, Ref. 23). The plot T/X versus T for the resistive transition of the sample Bi-2212 $_{0.8}$ (Fig. 1, inset) is illustrated in Fig. 1. The linear dependence is clearly borne out between approximately 84 and 89 K, signaling the 2D-layer behavior predicted by Monte Carlo simulations and renormalization-group analyses. The deviation above 89 K is probably due to the amplitude fluctuations of the order parameter. Equation (2) and the extrapolation from Fig. 1 lead to $T_{c0} = 91.5$ K. The definition of the variable X shows that the critical temperature in the case of decoupled layers would be $T_c = T_{c2D} = 78.9$ K [$X(T_{c2D}) = 1$, see Fig. 1]. T_{c2D} is the T_{KT} value of the layered system without interlayer coupling [Eq. (1)]. The 2D-layer behavior ends, however, at a certain temperature $T^* \approx 84$ K (Fig. 1). This is because for $T < T^*$ the interlayer Josephson coupling sets in, as shown below, and this will inhibit the pure 2D vortex fluctuations in the superconducting layers.

There are several approaches concerning the occurrence of finite resistivity in the limit of small transport currents in thin film samples. The low-current ohmic $V(I)$ signal in ultrathin YBaCuO films was attributed to the vanishing of the logarithmic interaction between vortices and antivortices at large separations,²⁴ which can lead to the existence of free vortices at all temperatures, in the absence of relevant pinning. Such free vortices should generate Arrhenius behavior in the $\rho(T)$ plot, but, as shown in Fig. 2(a), this is not the case for our Bi-2212 $_{0.8}$ sample. However, this effect, as well as finite size effects,¹ will turn an eventual BKT transition into a crossover, because the free vortices screen the vortex interaction better than do pairs, and thus make vortex pair unbinding possible at lower temperatures.

The renormalization-group analysis performed in Refs. (17) and (18) revealed that just above the resistive transition the superconducting layers decouple, at large length scales first. [The layers will be decoupled at all lengths above a temperature value higher than the critical temperature (for our sample, above T^*).] Thus, the linear $V(I)$ signal at low I values for T below T^* can be caused by free 2D vortices appearing in the superconducting layers at large probing lengths. However, in such a situation, it would be difficult to explain the finite voltage detected just above the zero-field transition temperature in transport measurements in the so called “transformer” electrode geometry.²⁵

Finally, since the real T_c of the system is lower than T^* (Fig. 1), it is natural to take into consideration the 2D-film behavior, related to vortex-string excitations. The vortex-gas-Coulomb-gas analogy predicts for $\rho(T)$ in the vicinity

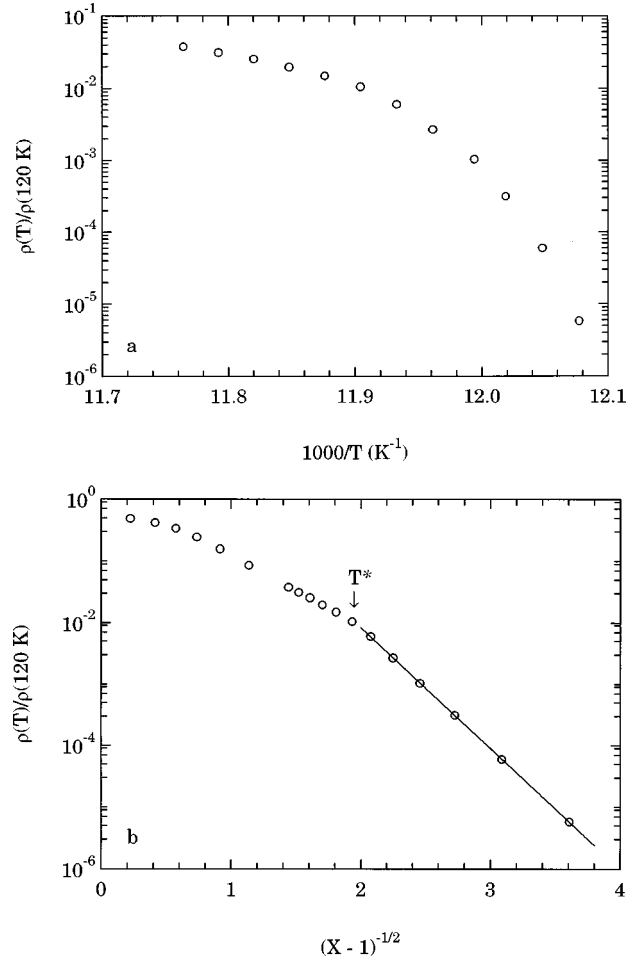


FIG. 2. (a) The downward curvature in the Arrhenius plot of the resistivity indicates a minor contribution of size effects in our samples (see text). (b) Temperature variation of the reduced resistivity fitted at low levels with Eq. (3) (sample Bi-2212 $_{0.8}$, $T_c = 82.2$ K, $C = 4.5$). The resistivity was determined from the linear part of the I - V curves, in the low- I limit (Fig. 3).

of T_c a dependence similar to that expected in the case of a BKT transition in the critical region

$$\rho(T) \sim \exp[-C(X-1)^{-1/2}], \quad (3)$$

with $C = \text{const}$. This is illustrated for the sample Bi-2212 $_{0.8}$ in Fig. 2(b), with a critical temperature $T_c = 82.2$ K and $C = 4.5$. In order to avoid the complications that may arise from the change of the probing length with temperature [when measuring $\rho(T)$ at constant current], for the plots in Figs. 2(a) and 2(b) the resistance was determined from the linear part of the I - V curves in the limit of small transport currents observed for $T > T_c$ (Fig. 3). The T^* value appearing in Fig. 2(b) is practically identical to that from Fig. 1. The agreement between the data just above T_c and Eq. (3) suggests that, in the conditions of negligible pinning and minor size effects, the resistive transition may be in connection with the 2D-film behavior,^{11,12} i.e., to be caused by the dissociation of vortex-string-antivortex-string pairs.

The change of the I - V curve shape with decreasing temperature below T_{c0} supplies new useful information. The representative I - V curves of the oxygen annealed film measured in a magnetically shielded environment are illustrated

in Fig. 3. A few characteristic temperature regions can be observed. In the first one (I), for T higher than T^* , the I - V curves are ohmic practically for all used current values, which is in agreement with the 2D-layer behavior of the $\rho(T)$ variation (Fig. 1). In this temperature interval, the 2D vortex-antivortex correlation length is small, since T^* is significantly higher than T_{c2D} . In the second temperature region (II), situated below T^* , the I - V curves are linear in the limit of small transport currents, but exhibit a downward curvature in the double logarithmic plot at higher currents. In region III, below T_c (but not very close to it), the negative curvature is present in the whole investigated current-voltage range. For the as-grown sample, the curvature is less pronounced and the temperature region III is narrow.²⁰ In region IV, the downward curvature in the double logarithmic plot disappears in the sensitivity window of our experiments. All these features will be discussed below, emphasizing the importance of the probing length imposed by the value of the current-density in transport measurements.

At least for highly anisotropic Bi-based and Tl-based HTSC's, the 2D-layer case (decoupled layers) represents a good starting approximation and it will be shortly summarized here. The energy of a 2D vortex pair of separation r in the presence of a transport current density J flowing parallel to the (a, b) plane is^{1,7}

$$E(r) \approx 2E_c + E_1 \ln(r/\xi) - s\Phi_0 J r, \quad (4)$$

where E_c is the creation energy and ξ is the coherence length in the (a, b) plane. The second term on the right-hand side of Eq. (4) is the usual logarithmic interaction. $E_1 = s\Phi_0^2/2\pi\lambda^2\varepsilon\mu_0$ is the coupling constant in the (a, b) plane. The third term represents the modification of the interaction energy due to the Lorentz force. The pair energy has a maximum for a separation r_m given by

$$r_m = E_1/s\Phi_0 J. \quad (5)$$

The density of unbound vortices can be determined by the balance between the rate of production and the rate of recombination. For a system of large extension, the form of the low voltage level I - V curves was derived²⁶ by considering a classical escape over the barrier $\Delta E = E(r_m) - 2E_c$, and the Bardeen-Stephen model for the flux flow resistance. Considering the transport current $I = JS$, where S is the sample cross section, this leads to

$$V \sim I^\alpha, \quad (6)$$

with the exponent

$$\alpha = 1 + E_1/2k_B T. \quad (7)$$

Recent Langevin simulations of 2D vortex fluctuations¹⁰ pointed out that due to an anomalous diffusion and the $1/t$ tail of the vortex correlations, the above classical prediction is no longer correct. The I - V characteristics remain of the form given by relation (6) at low driving forces, but a scaling argument suggests that the exponent consistent with the $1/t$ tail is

$$\beta = 2\alpha - 3 = E_1/k_B T - 1 = s\Phi_0^2/[2\pi\lambda^2(T)\varepsilon(T)\mu_0 k_B] - 1. \quad (8)$$

For finite interlayer Josephson coupling (quasi-2D case), in the simple single-pair model,⁷ the pair energy at large vortex-antivortex separations appears to be of the form

$$E(r) \approx 2E_c + E_1 \ln(r/\xi) + E_2(r/\xi) - s\Phi_0 J r. \quad (9)$$

The third term has its origin in the interlayer Josephson coupling, but takes the above linear form only for separations much larger than the Josephson length $\lambda_J = \gamma s$ (where γ is the anisotropy parameter). For separations smaller than the Josephson length, this term is negligible.¹ The coupling constant $E_2 = E_1 \xi/\lambda_J$. The pair energy from Eq. (9) has its maximum value for a separation r_m given now by $r_m = E_1/(s\Phi_0 J - E_2/\xi)$. r_m would be an appropriate probing length in transport measurements, since the vortices created at a separation larger than r_m will contribute to dissipation. However, as pointed out in Ref. 27, by taking into account the entropy gain at the current-induced vortex-antivortex unbinding below T_c , the value of this critical separation will be reduced. It becomes

$$r_c = (E_1 - Kk_B T)/[s\Phi_0(J - J_c)], \quad (10)$$

where the parameter $K \approx 4$ for pairs of large separations (of the order of the characteristic sample size), whereas for very small pairs $K \approx 2$. Equation (9) shows that the current induced vortex-antivortex unbinding is possible only for transport current densities greater than a critical value

$$J_c = E_2/s\Phi_0 \xi = \Phi_0/[2\pi\lambda^2(T)\varepsilon(T)\mu_0 \gamma s]. \quad (11)$$

The renormalization of the interlayer coupling leads, however, to a J_c value significantly lower than that predicted by the above model.^{16,17} It is worth noting that a bound quasi-2D vortex pair is a vortex loop threading one $(\text{CuO}_2)_2$ layer only. Such a vortex loop is composed of a pair of 2D vortices connected by interlayer vortex segments parallel to the (a, b) plane. [We consider the intermediate situations, with vortex loops threading many $(\text{CuO}_2)_2$ layers, but closing inside the sample, not relevant for our thin film samples.¹¹] The nonzero critical-current density appears from the fact that a minimum current is needed to overcome the in-plane attraction due to the Josephson coupling between the layers. Following the widely used derivation,^{26,7} in the quasi-2D case the I - V curve will take the form

$$V \sim I(I - I_c)^{\alpha-1}, \quad (12)$$

where the exponent α is the same as in the pure 2D case. Here $I_c = J_c S$ is the critical current. With the findings from Ref. 10, if one considers the quasi-2D situation, the I - V curves will have the form given by Eq. (12), but the expected exponent should be β from Eq. (8) instead of α [Eq. (7)].

As illustrated in Fig. 3, in region III, at low temperatures, the I - V curves of our samples can be fitted with Eq. (12), in a three parameter fit. The same fit was also possible in the case of the as-grown film, but only in a narrow temperature interval. In the vicinity of T_c , in both regions II and III, a good fit of the I - V curves with Eq. (12) can still be obtained, if some data at low voltages are not taken into account.⁸ Besides some inhomogeneities in the interlayer Josephson coupling across the sample, as well as size effects,^{1,24} this can be understood if one considers the vortex-string excitation at large length scales. As discussed in Ref. 8, the exci-

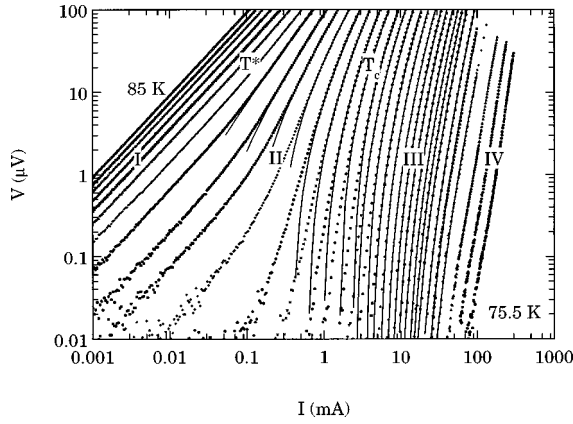


FIG. 3. Zero-field I - V curves of the oxygen annealed film (Bi-2212 ox). From left to right: T (K)=75.5, 76.5, 77.5, 78.5, 79, 79.4, 79.8, and from 80 K up to 85 K in steps of 0.2 K. The continuous lines represent the fit of the I - V curves with Eq. (12) (three parameter fit). I, II, III, and IV are the characteristic regions discussed in text. The layer decoupling temperature T^* and the critical temperature T_c are also indicated.

tation of vortex-string pairs threading the whole film (with logarithmic interaction only) becomes favored close to T_c and for large vortex-antivortex separations. In other words, the quasi-2D vortex loops will blow out along the c direction at large intervortex distances. For the thin film samples investigated by us, in the sensitivity window of our experiments, the occurrence of finite resistance above T_c in the limit of small transport currents seems to be mainly related to the vortex-string pair dissociation.^{11,12} This is supported not only by the $\rho(T)$ variation illustrated in Fig. 2(b), but also by the power-law dependence of the I - V curves appearing at low voltage levels just below T_c (see Fig. 3). However, it is worth noting that an exponent equal to 3 appears at $T=82.6$ K, which is slightly higher than the T_c value extracted from the fit of the resistive data [82.2 K, Fig. 2(b)]. The difference can result from the superposition of some quasi-2D vortex unbinding signal over the voltage signal given by the vortex-string unbinding.

Just above T_c , the I - V curves are linear at small transport currents [large probing lengths, see Eq. (5)], but exhibit a downward curvature in the double logarithmic plot at high currents [i.e., at smaller probing lengths, Eq. (10)]. In the latter case, the dissipation results from the unbinding of quasi-2D pairs, since the layers are still coupled at short lengths,^{17,18} and one can fit the data with Eq. (12). The ohmic behavior at small currents is generated by the existence of free vortices at large probing lengths. Taking into account the above interpretation of the resistive transition, in terms of vortex-string pair dissociation, and the shape of the low-voltage level I - V curves just below T_c , the free vortices for $T_c \leq T < T^*$ should be vortex strings. One can check this possibility by comparing the BKT correlation length of the 2D vortices in the $(CuO_2)_2$ layers, ξ_{+2D} , and that for vortex strings, $\xi_{+string}$, with the correlation length representing the scale above which the layers are decoupled, in the sense discussed in Ref. (18). The latter is $l \sim (T/T_c - 1)^{-2}$. Since above T^* the layers are decoupled at all lengths, $l(T^*)$ must be of the order of λ_J (≈ 150 nm for our Bi-2212 ox sample, see below). By considering for ξ_{+2D} and $\xi_{+string}$ the interpo-

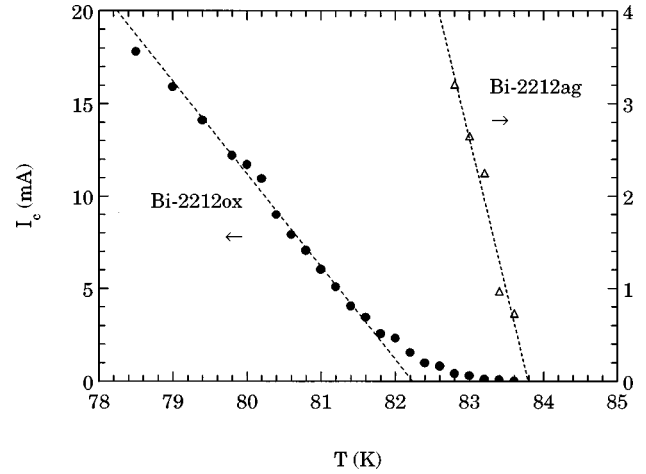


FIG. 4. Temperature dependence of the zero-field critical current extracted from the fit of the I - V curves with Eq. (12). The dashed lines are the linear fits of the data not very close to the layer decoupling temperature T^* .

lation formula from Ref. 21, with T_{c2D} and T_c from Fig. 1, it results $\xi_{+string} > l > \xi_{+2D}$. In these circumstances, the 2D vortices free of any in-plane interaction (which would appear at length scales larger than l) located in different $(CuO_2)_2$ layers can align, forming vortex strings, because the layers are still coupled at short scales. The presence of vortex strings explains not only the $\rho(T)$ dependence as illustrated in Fig. 2(b), but also the occurrence of a finite secondary voltage just above T_c in transport measurements with a ‘‘flux transformer’’ electrode geometry.²⁵

The critical current determined from the fit is plotted in Fig. 4. I_c vanishes practically at T^* , meaning that this is the layer decoupling temperature. Above T^* , the vortex strings cannot survive,²⁸ and the 2D-layer behavior can be observed (Fig. 1). Not very close to T^* , the $I_c(T)$ variation is linear (Fig. 4). Such a temperature dependence was already extracted¹⁷ from a self-consistent study of the effect of a current on the behavior of vortices in layered systems, using a renormalization-group analysis. Considering Eq. (11), one has, roughly, $dI_c/dT \sim 1/\gamma$, and the data plotted in Fig. 4 indicate that after the performed oxygen annealing the anisotropy parameter decreased by a factor of 2. With the γ value of the as-grown film estimated in Ref. 29, this leads to an anisotropy parameter for Bi-2212 ox of the order of 100.

At low temperatures and/or higher currents, the downward curvature in the log-log plot disappears (region IV, Fig. 3). This crossover from quasi-2D to 2D-layer behavior was clearly observed for similar samples with a reduced cross section, for which large transport current densities can be attained without heating problems.³⁰ The data from Fig. 3 show that it is not simply the consequence of the form of the I - V curve [Eq. (12)], which, for $I \gg I_c$, transforms into a power-law dependence [Eq. (6)]. The reentrant 2D behavior of the I - V curves appears at lower currents, and can be explained as follows. The density of thermally excited vortex pairs and the mean separation between paired vortices decrease with decreasing temperature. Consequently, in order to have a detectable voltage, a higher current density is needed at low temperatures, which means a reduction of the probing length. Neglecting pinning and self-field effects, one

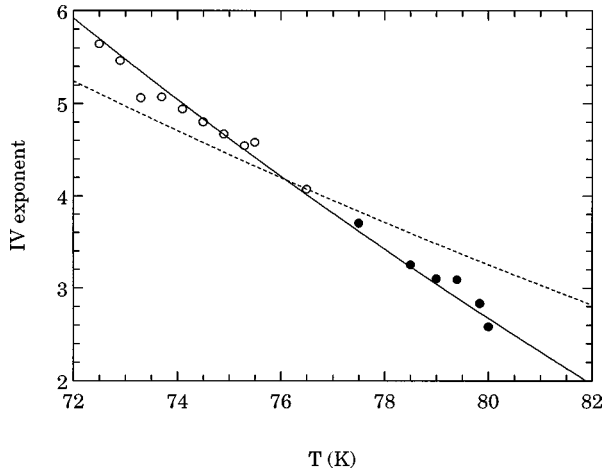


FIG. 5. Temperature dependence of the 2D I - V exponent (●): I - V exponent values resulting from the fit of the I - V curves in region III with Eq. (12) (see Fig. 3); (○): I - V exponent determined as the slope of the I - V curve in the log-log plot in region IV. The continuous line and the dashed line are the fit with Eqs. (8) and (9), respectively.

enters region IV, from above, when the probing length becomes lower than λ_J . Below this length, the term in the pair energy given by the interlayer coupling is insignificant. In this sense, one expects reentrant 2D-layer behavior in highly anisotropic HTSC's at low temperatures and/or high current densities. [A close inspection of the data from Fig. 3 shows that in region IV, at low temperatures (i.e., high current levels), the I - V curves exhibit a very slight upward curvature. This seems to be mainly a self-field effect.] For a quantitative estimation, one can use Eq. (10) for r_m as probing length, with $K \approx 3$ for pairs of separations $\approx \lambda_J$. As can be seen from Fig. 5, at a temperature value around 78–79 K, for example, the I - V exponent is ≈ 3 . With Eq. (8) and a γ value ≈ 100 , the condition $r_c \approx \gamma s$ ($s = 1.5$ nm) predicts reentrant 2D-layer behavior for the Bi-2212ox sample when I - I_c is of the order of 10^2 mA, in agreement with the experimental observation (Fig. 3).

As shown above, the classical approach⁹ and recent simulations of the Coulomb gas model¹⁰ offer different solutions for the I - V exponent [Eqs. (7) and (8), respectively]. In order to diminish the influence of the spatial renormalization on the I - V exponent value,²⁶ the modification of the vortex-antivortex interaction energy with the intervortex distance, as well as self-field effects, one has to consider the voltage from a limited current interval. In the case of sample Bi-2212ox, for I between approximately 50 and 150 mA, for example, the I - V exponent resulting from the fit of the I - V curves with Eq. (6) in region IV and with Eq. (12) in region III is illustrated in Fig. 5. We obtained a good agreement with the anomalous exponent suggested by Langevin simulations of 2D vortex fluctuations. The fit of the data with Eq.

(8) [one parameter fit, with $T_{c0} = 91.5$ K and $\varepsilon(T) = 1$] leads to $\lambda(0) = 155$ nm [considering $\lambda(T) = \lambda(0)(1 - T/T_{c0})^{-1/2}$], which is very close to the widely accepted value for Bi-2212.¹ Finally, we note that there is a good correspondence between the 2D-layer behavior observed in region I and in region IV. The value of the I - V exponent at $T = T_{c2D}$ is ≈ 3 (Fig. 5).

IV. CONCLUSIONS

The resistive transition and the changes in the shape of the I - V curves of high-quality Bi-2212 films observed by decreasing the temperature below T_{c0} in zero applied magnetic field can be satisfactorily explained in terms of vortex-fluctuations-induced layer decoupling and vortex-antivortex unbinding, showing a strong probing length dependence. The characteristic regions appearing in the current-temperature diagram are in close connection with the effective dimensionality of thermally excited vortices involved in the dissipation process. Above a temperature value $T^* < T_{c0}$, the I - V curves are linear for a large current-density interval, and the resistivity exhibits 2D-layer behavior, reflecting the occurrence of layer decoupling, as suggested by Monte Carlo simulations and renormalization group analyses. In the sensitivity window of our experiments, finite resistance in the limit of small transport currents appears at a temperature T_c lower than T^* , mainly through the dissociation of vortex-string-antivortex-string pairs. Below T_c , in a temperature interval whose extension depends on anisotropy, the voltage is generated by the current induced unbinding of quasi-2D vortex pairs, and the I - V curves can be fitted with the expression $V(I) \sim I(I - I_c)^{\beta-1}$. The deviation at low voltage levels close to T_c was explained through the contribution of thermally excited vortex strings. It was found that the slope dI_c/dT increases after oxygen annealing, which supports the idea that the finite zero-field critical current results from the interlayer Josephson coupling. At low temperatures and/or high transport current densities, we observed a crossover from quasi-2D to 2D-layer behavior, due to the decrease of the probing length below the Josephson length, where the Josephson coupling becomes irrelevant. The reentrant 2D-layer behavior of the I - V curves covers a large portion of the current-temperature diagram of highly anisotropic HTSC's in zero external magnetic field. The determined temperature variation of the 2D I - V exponent is in agreement with the result of recent Langevin simulations of the Coulomb-gas model.

ACKNOWLEDGMENTS

This work was supported by the Deutsche Forschungsgemeinschaft through Sonderforschungsbereich 262. L.M. wishes to acknowledge the kind assistance of the Alexander von Humboldt Foundation and to thank P. Minnhagen and S. W. Pierson for stimulating discussions.

*Permanent address: Institute for Materials Physics, Bucharest, P.O. Box MG-7, Romania.

¹G. Blatter, M. G. Feigel'man, V. B. Geshkenbein, A. I. Larkin, and V. M. Vinokur, Rev. Mod. Phys. **66**, 1125 (1994), and references therein.

²S. Martin, A. T. Fiory, R. M. Fleming, G. P. Espinosa, and S. A. Cooper, Phys. Rev. Lett. **62**, 677 (1989); D. H. Kim, A. M. Goldman, J. M. Kang, and R. T. Kampwirth, Phys. Rev. B **40**, 8834 (1989); P. C. E. Stamp, L. Forro, and C. Ayache, *ibid.* **38**, 2847 (1988); N. -C. Yeh and C. C. Tsuei, *ibid.* **39**, 9708 (1989);

- S. N. Artemenko, I. G. Gorlova, and Yu. I. Latyshev, *Pis'ma Zh. Eksp. Teor. Fiz.* **49**, 566 (1989) [*JETP Lett.* **49**, 654 (1989)].
- ³V. L. Berezinskii, *Zh. Eksp. Teor. Fiz.* **61**, 1144 (1971) [*Sov. Phys. JETP* **34**, 610 (1972)]; J. M. Kosterlitz and D. J. Thouless, *J. Phys. C* **6**, 1181 (1973); J. M. Kosterlitz, *ibid.* **7**, 1046 (1974).
- ⁴M. R. Beasley, J. E. Mooij, and T. P. Orlando, *Phys. Rev. Lett.* **42**, 1165 (1979).
- ⁵L. I. Glazman and A. E. Koshelev, *Zh. Eksp. Teor. Fiz.* **97**, 1371 (1990) [*Sov. Phys. JETP* **70**, 774 (1990)]; S. Hikami and T. Tsuneto, *Prog. Theor. Phys.* **63**, 387 (1980).
- ⁶V. Cataudella and P. Minnhagen, *Physica C* **166**, 442 (1990).
- ⁷H. J. Jensen and P. Minnhagen, *Phys. Rev. Lett.* **66**, 1630 (1991).
- ⁸L. Miu, P. Wagner, U. Frey, A. Hadish, D. Miu, and H. Adrian, *Phys. Rev. B* **52**, 4553 (1995).
- ⁹D. R. Nelson and J. R. Kosterlitz, *Phys. Rev. Lett.* **39**, 1201 (1977); V. Ambegaokar, B. I. Halperin, D. R. Nelson, and E. Siggia, *ibid.* **40**, 783 (1978); *Phys. Rev. B* **21**, 1806 (1980), V. Ambegaokar and S. Teitel, *ibid.* **19**, 1667 (1979); B. I. Halperin and D. R. Nelson, *J. Low Temp. Phys.* **36**, 599 (1979).
- ¹⁰K. Holmlund and P. Minnhagen, *Phys. Rev. B* **54**, 523 (1996).
- ¹¹Y. Matsuda, S. Komiyama, T. Onogi, T. Terashima, K. Shimura, and Y. Bando, *Phys. Rev. B* **48**, 10 498 (1993).
- ¹²T. Ota, I. Tsukada, I. Terasaki, and K. Uchinokura, *Phys. Rev. B* **50**, 3363 (1994).
- ¹³H. Weber and H. J. Jensen, *Phys. Rev. B* **44**, 454 (1991); P. Minnhagen and P. Olsson, *ibid.* **44**, 4503 (1991).
- ¹⁴P. Minnhagen and P. Olsson, *Phys. Rev. Lett.* **67**, 1039 (1991).
- ¹⁵M. Friesen, *Phys. Rev. B* **51**, 632 (1995).
- ¹⁶S. W. Pierson, *Phys. Rev. Lett.* **73**, 2496 (1994).
- ¹⁷S. W. Pierson, *Phys. Rev. Lett.* **74**, 2359 (1995).
- ¹⁸S. W. Pierson, *Phys. Rev. B* **54**, 688 (1996).
- ¹⁹S. E. Korshunov, *Europhys. Lett.* **11**, 757 (1990); B. Horovitz, *Phys. Rev. Lett.* **67**, 378 (1991).
- ²⁰P. Wagner, F. Hillmer, U. Frey, and H. Adrian, *Phys. Rev. B* **49**, 13 184 (1994).
- ²¹P. Minnhagen, *Rev. Mod. Phys.* **59**, 1001 (1987).
- ²²V. Persico, V. Cataudella, F. Fontana, and P. Minnhagen, *Physica C* **260**, 41 (1996).
- ²³P. Minnhagen and P. Olsson, *Phys. Scr.* **T42**, 9 (1992).
- ²⁴J. M. Repaci, C. Kwon, Q. Li, X. G. Jiang, T. Venkatesan, R. E. Glover III, C. J. Lobb, and R. S. Newrock, *Phys. Rev. B* **54**, R9674 (1996).
- ²⁵Y. M. Wan, S. E. Hebboul, D. C. Harris, and J. C. Garland, *Phys. Rev. Lett.* **71**, 157 (1993).
- ²⁶A. M. Kadin, K. Epstein, and A. M. Goldman, *Phys. Rev. B* **27**, 6691 (1983).
- ²⁷L. Miu, *Phys. Rev. B* **50**, 13 849 (1994).
- ²⁸K. H. Fischer, *Physica C* **210**, 179 (1993), and references therein.
- ²⁹L. Miu, P. Wagner, A. Hadish, F. Hillmer, and H. Adrian, *Physica C* **234**, 249 (1994).
- ³⁰L. Miu *et al.* (unpublished).